

## VISCO-ELASTIC FLUID MODEL IN AN INCLINED POROUS STENOSED ARTERY WITH SLIP EFFECT AND BODY ACCELERATION

Rana MANISHA\* and Surendra KUMAR  
University Institute of Engineering and Technology,  
Maharshi Dayanand University, Haryana, INDIA  
E-mail: manisharana88@gmail.com

The present paper analyzes an unsteady magnetohydrodynamic blood flow model of an visco-elastic fluid through an inclined porous stenosed artery with body acceleration and slip effect. Navier-Stokes equations have been used to describe the blood flow model. The governing equation of blood flow is solved by an analytic method by considering blood as an incompressible, visco-elastic fluid, and suspension of RBC's in plasma. Axial velocity, blood acceleration, flow rate, and shear stress are derived numerically by using the finite Laplace and Hankel transformation and their inverse. The effect of parameters such as the visco-elasticity parameter, Womersley number, Hartmann number, inclination angle, parameter of slip, and body acceleration frequency is analyzed. Axial velocity reduces as the Hartmann number and visco-elasticity parameter enhance and it enhances with the enhancement of the slip parameter and inclination angle. The study is beneficial for finding the effect of slip parameter, porosity factor and Hartmann number when a human body is exposed to MRI and CT scan.

**Key words:** visco-elastic fluid, slip condition, inclined porous artery, permeability, body acceleration.

### 1. Introduction

Nowadays, cardiovascular diseases have a great effect on human beings all over the world. Diseases like heart failure, heart attack, brain stroke, narrowing of the artery, etc., are the main cause of death in the young population of the earth. The narrowing of the artery is medically termed as stenosis. Stenosis disturbs the characteristics of blood flow in the human artery. Mathematical studies of blood flow past an inclined stenosed, bifurcated and tapered are of great significance. It is usually known that tubes are not horizontal in physiological systems but have some inclination to the axis. Chakraborty *et al.* [15] presented a blood flow model past an inclined artery with radially symmetric but axially non-symmetric stenosis. They illustrated that flow resistance enhances with the stenosis size and hematocrit but it reduces with the inclination angle and slip at the wall. Tripathi [17] examined a blood flow model past an inclined artery with the impact of a magnetic field by describing blood as a couple stress fluid. They detected that axial velocity enhances with the augmentation of the couple-stress parameter. Srivastava [23] studied flow characteristics of an MHD blood in an inclined porous stenosed artery with the effect of an inclined magnetic field. Kumar *et al.* [25] analyzed a blood flow model past a tapered inclined artery under the impact of a magnetic field and in a porous medium. They found that shear stress magnifies with the augmentation of the inclination angle of the artery. Sharma *et al.* [26] evaluated the effect of overlapping stenosis and dilatation in an inclined artery with the non-Newtonian blood flow. They discovered that fluid velocity decreases in the area of dilatation and skin friction increases at the extremities of the overlapping stenosis. Kumari *et al.* [28] studied an unsteady MHD fluid with peristaltic transport with a slip effect past an inclined stenosed artery.

A porous medium is made of a solid matrix and interconnected void. The porosity is defined as the ratio of void space to total volume. The permeability of a porosity of the medium represents the flow conductivity in the medium. The impact of the magnetic field and porous medium is the concern of numerous applications in recent years. The red blood cells are a vital bio-magnetic material and the blood flow can be

---

\* To whom correspondence should be addressed

affected by the magnetic field. Tzirtzilakis [6] presented a blood flow model with the impact of a magnetic field. This blood flow model is based on the principle of magnetohydrodynamics, the fluid's magnetic property and electrical conductivity of blood. Verma and Parihar [12] analyzed the blood flow model in multi-stenosis arteries in the presence of a magnetic field. This model is based on the principles of ferrohydrodynamics and MHD. The outcomes show that for a weak heart low diastolic pressure and high systolic pressure are very harmful. Sinha *et al.* [14] evaluated the blood flow in a porous artery with double stenose under the impact of a magnetic field. They revealed that the flow rate magnifies with the enhancement of velocity slip. Eldesoky [16] analyzed the slip effect of magnetohydrodynamics pulsatile blood flow with the influence of body acceleration. He showed that the flow is greatly affected by the Knudsen number of slip, magnetic field and body acceleration frequency. An unsteady pulsatile blood flow in a porous stenotic artery in the presence of a magnetic field is reported by Sharma *et al.* [18]. They found that both porosity and magnetic field decrease the blood transported to the organs. Sharma *et al.* [20] evaluated an MHD pulsatile blood flow in the arteries with the double stenoses. They found that fluid velocity reduces when the magnitude of the Hartmann number enhances and shear stress amplifies when the Hartmann number magnifies.

Beaver and Joseph [2] and Saffman [3] explored the properties of flow of blood across a constricted artery by considering boundary and slip conditions at the permeable vessel. Chaturani and Biswas [4] examined the Poiseuille flow of a polar fluid with various boundary conditions, namely: couple stress zero or non-zero and slip or no-slip at the wall. The slip effects for a non-Newtonian Maxwellian fluid on the peristaltic flow in porous media was studied by El-Shehawey *et al.* [7]. They revealed that the net flow rate is strongly influenced by the Knudsen number of slip flow and a non-Newtonian nature of the fluid. Ponalagusamy [8] studied the two-layered motion of blood past a mild stenosis artery with variable slip and peripheral layer thickness by describing blood as a Newtonian. Hayat *et al.* [10] discussed that slip effects on the viscous fluid with peristaltic flow in a porous medium. Nadeem and Akram [13] discussed the slip effects of an asymmetric channel with a Jeffrey fluid with the impact of a magnetic field. They found that temperature field reduces with the enhancement of the slip parameter and Jeffrey parameter. Sinha *et al.* [19] examined the influence of slip on flow of blood in a constricted artery under the impact of body acceleration. They showed that flow resistance enhances with the stenosis height increase and velocity slip increase. Sharma *et al.* [22] considered an MHD pulsatile flow in a catheterized narrow artery with a slip on the wall. They observed that WSS magnifies with the enhancement of the transverse magnetic field.

Many studies have been denoted to examine the effect of a porous medium with body acceleration. The blood flow is disturbed when there is a sudden change in the human body. Although the human body was adapted to these sudden changes, the changes may result in many health diseases. In many circumstances like travel in vehicles, spacecraft, aircraft, sports activities, etc. the human body is exposed to vibrations and they can be the cause of severe health risk factors namely, enhancing rate of pulse, blurred vision, stomachache, and headache. El-Shehawey *et al.* [5] studied a magnetohydrodynamic flow of an visco-elastic fluid under the effect of body acceleration. They obtained the numerical derivation of flow rate, shear stress, fluid acceleration and axial velocity. Nagarani and Sarojamma [9] investigated a pulsatile flow of a non-Newtonian fluid described by the Casson model through the mild stenosis artery under the impact of body acceleration. They revealed that the flow rate enhances in the existence of blood acceleration. A pulsatile blood flow in a porous narrow artery with the impact of body acceleration and magnetic field was analyzed by Rathod and Tanveer [11]. They found that the velocity enhances with the enhancement of body acceleration and permeability parameter while it reduces as the magnetic parameter magnifies. The parameter of slip at walls in a unsteady MHD blood flow model was analyzed by Eldesoky [21]. He revealed that blood axial velocity reduces at the neck of the stenosis with the augmentation of the slip parameter. Sharma *et al.* [24] studied the effect of axial translation, transverse magnetic field and hematocrit concentration on the pulsatile blood flow past a narrowing artery. They demonstrated that fluid velocity enhances with the augmentation of the Reynolds number along the axial direction. Chitra and Karthikeyan [27] studied the impact of stenosis height on an MHD oscillatory blood flow in a tapered artery having inclination angle and detected that stenosis height outstandingly affects the shear stress. Manisha *et al.* [29] investigated the two-layered motion of blood flow in a porous narrowing artery with the impact of heat and mass transfer and a magnetic field. Jaafar *et al.* [30] presented a mathematical study of flow with chemical reaction in a stenosed artery. Shah *et al.* [31] examined the pulsatile MHD blood

flow in a porous tube of cylindrical shape with an inclined angle having generalized time-nonlocal shear stress. Manisha *et al.* [32] considered the blood flow model for various shapes of stenosis with the non-Newtonian power-law model. Manisha and Kumar [33] studied the non-Newtonian nature of blood described by the Casson model to show the effects of cosine shape stenosis in an artery.

It follows from the literature survey, that an visco-elastic fluid flow through a porous stenosed artery having an unsteady MHD effect, inclination angle, slip conditions, and body acceleration has not been studied yet. In the present manuscript, an unsteady MHD visco-elastic fluid model in an inclined porous stenosed artery having slip condition and body acceleration is analyzed. The study has been performed with the application of suitable analytical methods. This analysis helps to find the flow rate, blood acceleration, axial velocity, and shear stress in a specific situation.

## 2. Problem formulation

In the present study, blood is considered a suspension of red blood cells in plasma. Equation (2.1) represents the hematocrit concentration-dependent viscosity of blood [18].

$$\mu = \mu_0 \left[ 1 + \beta_1 h(r) \right]. \quad (2.1)$$

Here,  $\mu_0$  is the viscosity coefficient,  $\beta_1$  is a constant, and  $h(r)$  is the concentration of hematocrit varying along the radial direction represented as follows:

$$h(r) = Hm \left[ 1 - \left( \frac{r}{R_0} \right)^n \right] \quad (2.2)$$

where  $Hm$  represents the maximum concentration of hematocrit.

The mathematical representation of the geometry of the constricted arterial section is as follows:

$$R(z) = R_0 \left[ 1 - \frac{\delta}{2} \left( 1 + \cos \frac{\pi z}{L_0} \right) \right] \quad (2.3)$$

Here,  $R_0$  denotes the radius of the normal artery,  $R(z)$  denotes the radius of the stenosed artery,  $\delta$  is the maximum depth of the stenosis,  $2L$  denotes the length of the artery and  $2L_0$  denotes the length of the stenosis.

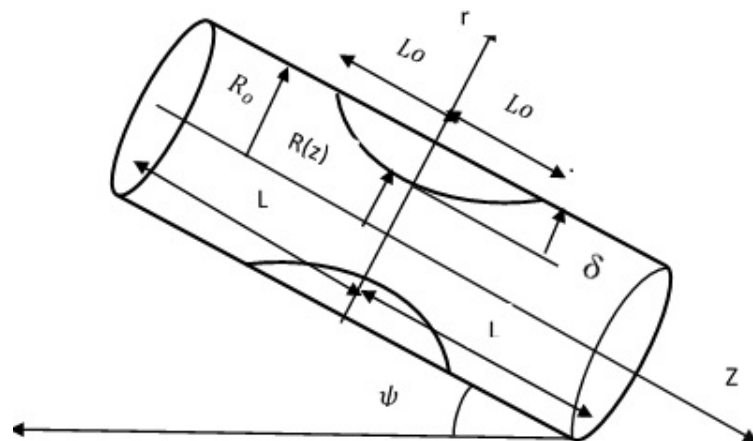


Fig.1. Geometry of cosine shape narrowing artery.

Consider a one-dimensional unsteady motion of an MHD blood flow through an inclined cylindrical stenosed artery with the effect of slip and blood acceleration. Blood is assumed to be an incompressible, visco-elastic fluid flowing in a porous medium which has permeability  $k$ . Blood is considered a non-Newtonian fluid with the electric conductivity in the presence of a transverse magnetic field. The applied magnetic field produces the electromotive force and this force is represented by Ohm's law as:

$$\mathbf{J} = \sigma(\mathbf{E} + \mathbf{q} \times \mathbf{B}). \quad (2.4)$$

The electro-magnetic force  $\mathbf{F}$  is:

$$\mathbf{F} = \mathbf{J} \times \mathbf{B} = \sigma(\mathbf{E} + \mathbf{q} \times \mathbf{B}) \times \mathbf{B}. \quad (2.5)$$

Here,  $\mathbf{E}$  indicates intensity of the electric field vector,  $\sigma$  is the defines electrical conductivity,  $\mathbf{q} = (0, 0, u)$  is the velocity vector,  $\mathbf{J}$  is the density of current, and  $\mathbf{B} = \mathbf{B}_0 + \mathbf{B}_I$  represents the intensity vector of the magnetic flux in which  $\mathbf{B}_I$  is a negligibly small vector of the induced magnetic field and  $\mathbf{B}_0$  is externally applied magnetic field. The vector  $\mathbf{E} = 0$  because of the no polarisation of charge [1]. Now, the magneto-hydrodynamic force is,

$$\mathbf{F} = \mathbf{J} \times \mathbf{B} = -\sigma B_0^2 u \text{ where } |\mathbf{B}_0| = B_0. \quad (2.6)$$

### 3. Equation of motion

The Navier-Stokes equation of motion is given in [5] in the cylindrical polar coordinate as

$$\rho \frac{\partial u}{\partial t} = -\frac{\partial p}{\partial z} + \rho G(t) + \left( \mu + \mu_l \frac{\partial}{\partial t} \right) \left( \frac{\partial^2 u}{\partial r^2} + \frac{1}{r} \frac{\partial u}{\partial r} \right) - \frac{\mu}{k} u - \sigma B_0^2 u + \rho g \sin \psi \quad (3.1)$$

where

$$-\frac{\partial p}{\partial z} = p_0 + p_l \cos(w_p t), \quad t \geq 0,$$

and

$$G(t) = G_0 \cos(w_b t + \phi), \quad t \geq 0$$

where  $p_0$  is the magnitude of pressure gradient of steady portion,  $p_l$  denotes the magnitude of the pressure gradient for the oscillatory part,  $z$  is the axial direction,  $\mu_l$  is the coefficient of visco-elastic fluid.  $w_p = 2rf_p$  with  $f_p$  is the heart pulse frequency,  $G_0$  defines magnitude of body acceleration,  $w_b = 2rf_b$  with  $f_b$  denote the frequency of body acceleration,  $\phi$  denotes phase difference,  $\psi$  is the inclination angle of the artery and  $t$  denotes time.

Then, Eq.(3.1) becomes

$$\begin{aligned} \rho \frac{\partial u}{\partial t} = & p_0 + p_l \cos(w_p t) + \rho G_0 \cos(w_b t + \phi) + \\ & + \left( \mu + \mu_l \frac{\partial}{\partial t} \right) \left( \frac{\partial^2 u}{\partial r^2} + \frac{1}{r} \frac{\partial u}{\partial r} \right) - \frac{\mu}{k} u - \sigma B_0^2 u + \rho g \sin \psi. \end{aligned} \quad (3.2)$$

For a dimensionless process, we insert some dimensionless terms:

$$\begin{aligned} u' &= \frac{u}{w_p R_0}, & r' &= \frac{r}{R_0}, & L_0' &= \frac{L_0}{R_0}, & z' &= \frac{z}{R_0} p_0' = \frac{R_0 p_0}{w_p \mu}, & p_1' &= \frac{R_0 p_1}{w_p \mu}, \\ t' &= t w_p, & g' &= \frac{\rho g}{w_p R_0}, & k' &= \frac{k}{R_0^2}, & b &= \frac{w_b}{w_p}, & G_0' &= \frac{\rho R_0 G_0}{w_p \mu}. \end{aligned} \quad (3.3)$$

After applying non-dimensional terms and ignoring ‘’ sign, we get

$$\alpha^2 \frac{\partial u}{\partial t} = p_0 + p_1 \cos t + G_0 \cos(bt + \phi) + \left( I + \beta \frac{\partial}{\partial t} \right) \left( \frac{\partial^2 u}{\partial r^2} + \frac{1}{r} \frac{\partial u}{\partial r} \right) - \left( H^2 + \frac{1}{k} \right) u + g_0 \quad (3.4)$$

where  $\alpha = \sqrt{\frac{R_0^2 \rho w_p}{\mu}}$  is the Womersley parameter,  $H = \sqrt{\frac{R_0^2 \sigma B_0^2}{\mu}}$  is the Hartmann number,  $M = \sqrt{\frac{I}{k}}$  is the permeability parameter,  $\beta = \frac{\mu_l}{\mu} w_p$  is the non-dimensional parameter of visco-elasticity and  $g_0 = \frac{g' R_0^2 \sin \psi}{\mu}$ .

Furthermore, we consider that at  $t=0$  the blood flows through the artery by an instant pressure gradient that is shown as:

$$-\frac{\partial p}{\partial z} = p_0 + p_1 \quad (3.5)$$

For a porous medium with small permeability, the boundary condition investigated by Beavers and Joseph [2] was simplified by Saffman [3] as  $\frac{du}{dy} = \frac{\eta}{\sqrt{k}} u$  where  $\eta$  represents a constant whose value is based on the porous material properties and on its structure and  $k$  is the permeability parameter. This boundary condition holds for the MHD flow and unsteady flow [21]. The initial and boundary conditions of the above stated problem may be represented as

$$(i) \quad \frac{\partial u}{\partial r} = -h_1 u \text{ for } r = a \quad \text{and} \quad t \geq 0 \text{ (Slip condition)} \quad (3.6)$$

where

$$h_1 = -\frac{\eta}{R_0 \sqrt{k}}$$

represents the slip parameter and  $a = \frac{R(z)}{R_0} = R_1(z)$ ,

$$(ii) \quad u(r, 0) = \sum_{n=1}^{\infty} \frac{2h_1}{a} \cdot \frac{p_0 + p_1 + g_0 + G_0 \cos \phi}{(H^2 + M^2 + \lambda_n^2)(h_1^2 + \lambda_n^2)} \frac{J_0(r\lambda_n)}{J_1(a\lambda_n)} \quad \text{for} \quad 0 \leq r \leq a, \quad (3.7)$$

(iii)  $u(0, t)$  is finite.

After applying non-dimensional terms and ignoring ‘’ sign, the geometry of the constricted arterial section is represented as

$$R_l(z) = \left[ I - \frac{\delta}{2} \left( I + \cos \frac{\pi z}{L_0} \right) \right]$$

#### 4. Solution of the problem

Using the Laplace transformation on Eq.(3.2), we get:

$$\begin{aligned} \alpha^2 \left( \overline{su(r,s)} - u(r,0) \right) &= p_0 \left( \frac{I}{s} \right) + p_l \left( \frac{s}{I+s^2} \right) + G_0 \left( \frac{s \cos \phi - b \sin \phi}{s^2 + b^2} \right) + \\ &+ \left( \frac{d^2}{dr^2} + \frac{I}{r} \frac{d}{dr} \right) \left( \overline{u(r,s)} + \beta s \overline{su(r,s)} - \beta u(r,0) \right) - (H^2 + M^2) \overline{u(r,s)} + g_0 \left( \frac{I}{s} \right). \end{aligned} \quad (4.1)$$

Applying the Hankel transformation to Eq.(4.1), we have

$$\begin{aligned} (\alpha^2 s + H^2 + M^2 + \lambda_n^2 + \beta s \lambda_n^2) \overline{u(\lambda_n, s)} - (\beta \lambda_n^2 + \alpha^2) u(\lambda_n, 0) &= \\ = \left( (p_0 + g_0) \frac{I}{s} + p_l \left( \frac{s}{I+s^2} \right) + G_0 \left( \frac{s \cos \phi - b \sin \phi}{s^2 + b^2} \right) \right) \cdot \frac{a}{\lambda_n} J_l(a \lambda_n). \end{aligned} \quad (4.2)$$

From (4.2), we have,

$$\begin{aligned} \overline{u(\lambda_n, s)} &= \frac{I}{s+l} \left( \frac{p_0 + p_l + g_0 + G_0 \cos \phi}{(H^2 + M^2 + \lambda_n^2)} \right) \cdot \frac{a}{\lambda_n} J_l(a \lambda_n) + \\ &+ \frac{I}{(\alpha^2 + \beta \lambda_n^2)(s+l)} \left[ (p_0 + g_0) \frac{I}{s} + p_l \left( \frac{s}{I+s^2} \right) + \frac{G_0 (s \cos \phi - b \sin \phi)}{s^2 + b^2} \right] \cdot \frac{a}{\lambda_n} J_l(a \lambda_n). \end{aligned} \quad (4.3)$$

where  $\lambda_n$  are the zeros of Eq.  $\lambda J_0'(a\lambda) + h_l J_0(a\lambda) = 0$ ,  $J_0(r)$  and  $J_l(r)$  are the first kind Bessel functions and  $l = \frac{(H^2 + M^2 + \lambda_n^2)}{(\beta \lambda_n^2 + \alpha^2)}$ .

To find the expression of velocity of the fluid, employing the inverse of the Laplace and Hankel transform to Eq.(4.3.), we have

$$\begin{aligned}
u(r,t) = & \frac{2h_l}{a} \sum_{n=1}^{\infty} \frac{J_0(r\lambda_n)}{(h_l^2 + \lambda_n^2) J_0(a\lambda_n) (\alpha^2 + \beta\lambda_n^2)} \\
& \left[ \frac{p_0 + g_0}{l} + e^{-lt} \left( \frac{p_l + G_0 \cos \phi}{l} - \frac{p_l \cdot l}{l+l^2} - \frac{G_0(l \cos \phi + b \sin \phi)}{l^2 + b^2} \right) + \right. \\
& \left. + \frac{G_0(l \cos(bt + \phi) + b \sin(bt + \phi))}{l^2 + b^2} + \frac{p_l(l \cos t + \sin t)}{l+l^2} \right]. \tag{4.4}
\end{aligned}$$

The acceleration of the fluid is:  $F(r,t) = \frac{\partial u}{\partial t}$

$$\begin{aligned}
F(r,t) = & \frac{2h_l}{a} \sum_{n=1}^{\infty} \frac{J_0(r\lambda_n)}{(h_l^2 + \lambda_n^2) J_0(a\lambda_n) (\alpha^2 + \beta\lambda_n^2)} \\
& \left[ -le^{-lt} \left( \frac{p_l + G_0 \cos \phi}{l} - \frac{p_l \cdot l}{l+l^2} - \frac{G_0(l \cos \phi + b \sin \phi)}{l^2 + b^2} \right) + \right. \\
& \left. + \frac{G_0(-lb \sin(bt + \phi) + b^2 \cos(bt + \phi))}{l^2 + b^2} + \frac{p_l(-l \sin t + \cos t)}{l+l^2} \right]. \tag{4.5}
\end{aligned}$$

Similarly, the flow rate  $Q$  is derived as:  $Q(z,t) = 2\pi \int_0^a r u(r,t) dr$

$$\begin{aligned}
Q(z,t) = & 4\pi h_l \sum_{n=1}^{\infty} \frac{J_1(a\lambda_n)}{\lambda_n (h_l^2 + \lambda_n^2) J_0(a\lambda_n) (\alpha^2 + \beta\lambda_n^2)} \\
& \left[ \frac{p_0 + g_0}{l} + e^{-lt} \left( \frac{p_l + G_0 \cos \phi}{l} - \frac{p_l \cdot l}{l+l^2} - \frac{G_0(l \cos \phi + b \sin \phi)}{l^2 + b^2} \right) + \right. \\
& \left. + \frac{G_0(l \cos(bt + \phi) + b \sin(bt + \phi))}{l^2 + b^2} + \frac{p_l(l \cos t + \sin t)}{l+l^2} \right]. \tag{4.6}
\end{aligned}$$

Also, the shear stress is obtained as:  $\tau(r,t) = \mu \frac{\partial u}{\partial r}$

$$\begin{aligned}
\tau(r,t) = & \frac{2\mu h_l}{a} \sum_{n=1}^{\infty} \frac{-\lambda_n J_1(r\lambda_n)}{(h_l^2 + \lambda_n^2) J_0(a\lambda_n) (\alpha^2 + \beta\lambda_n^2)} \\
& \left[ \frac{p_0 + g_0}{l} + e^{-lt} \left( \frac{p_l + G_0 \cos \phi}{l} - \frac{p_l \cdot l}{l+l^2} - \frac{G_0(l \cos \phi + b \sin \phi)}{l^2 + b^2} \right) + \right. \\
& \left. + \frac{G_0(l \cos(bt + \phi) + b \sin(bt + \phi))}{l^2 + b^2} + \frac{p_l(l \cos t + \sin t)}{l+l^2} \right]. \tag{4.7}
\end{aligned}$$

### 5. Numerical result and discussion

Velocity, flow rate, blood acceleration and shear stress are derived numerically by solving the Navier-Stokes equations using the Laplace and Hankel transformation and their inverse. The expression of Eqs (4.4), (4.5), (4.6), and (4.7) have been used to execute the numerical codes in mathematical software MATLAB and to get the plots for the velocity field, blood acceleration, flow rate, and stress field. The computation has been done for various values of parameters such as to show their relative effects the slip parameter  $h_l$ , permeability parameter  $M$ , Womersley parameter  $\alpha$ , visco-elasticity parameter  $\beta$ , Hartmann number  $H$ , body acceleration frequency  $b$ , the inclined angle of arterial segment  $\psi$ , phase difference  $\phi$  and magnitude of body acceleration  $G_0$  on the velocity trends, blood acceleration trends, profile of the flow rate, and shear stress trends.

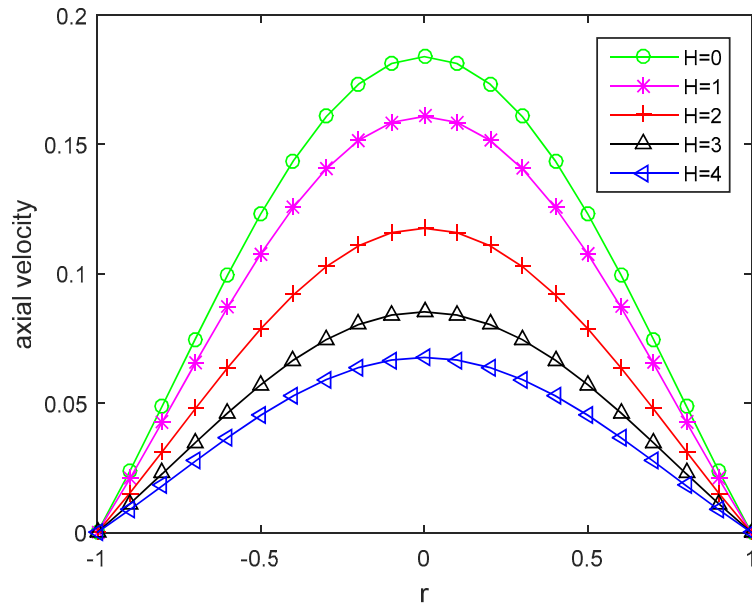


Fig.2. Plot of axial velocity versus  $r$  for the various values of the Hartmann number  $H$  and  $p_0 = 2, p_l = 4, G_0 = 2, h_l = 0.4, M = 1.5, t = 1, b = 2, a = 2, \psi = \pi / 3, \phi = 0.25$ .

Graphs of different physical quantities are plotted for different magnitude of  $p_0 = 2, p_l = 4, G_0 = 3, h_l = 0.4, M = 1.5, t = 1, b = 2, a = 2, \alpha = 2$ , and other different values of various parameters as used by other researchers [11, 16, 21, 25, 28]. The plot of axial velocity for various values of the parameters has been shown in Figs 2-8. The variation in axial velocity versus the radial distance of various values of the Hartmann number  $H$  and coefficient of visco-elasticity  $\beta$  is shown in Figs 2 and 3. The figures show that the flowing fluid decelerated slightly in the radial direction with the enhancement of the Hartmann number  $H$  and visco-elasticity parameter  $\beta$ . It has been observed that the velocity trend is almost flat for  $H = 4$  and  $\beta = 1$ . Moreover, it is also found that blood velocity is controlled by choosing appropriate values of the magnetic field parameter and visco-elasticity parameter. Figure 4 shows the changes in the axial velocity  $u(r,t)$  versus  $r$  for different values of the inclination angle  $\psi$ . The parabolic axial velocity profile gradually decreases when the inclination of the artery slightly enhances. Hence, the blood velocity is greatly affected by the stenosed artery inclination angle. The outcomes for velocity are in agreement with the results published [11, 16, 21, 25, 28].

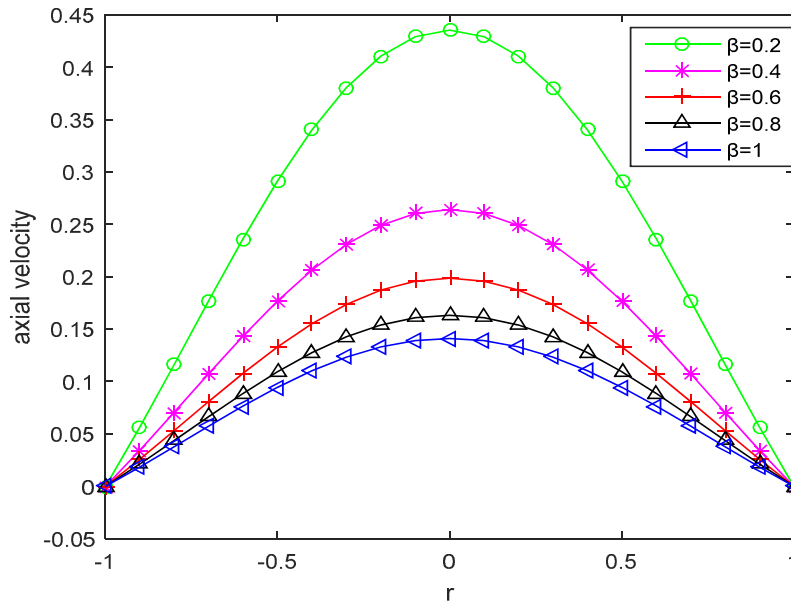


Fig.3. Plot of axial velocity versus  $r$  for various values of the visco-elasticity parameter  $\beta$  and  $p_0 = 2, p_1 = 4, G_0 = 2, h_1 = 0.4, M = 1.5, t = 1, b = 2, a = 2, \psi = \pi / 3, \phi = 0.25$ .

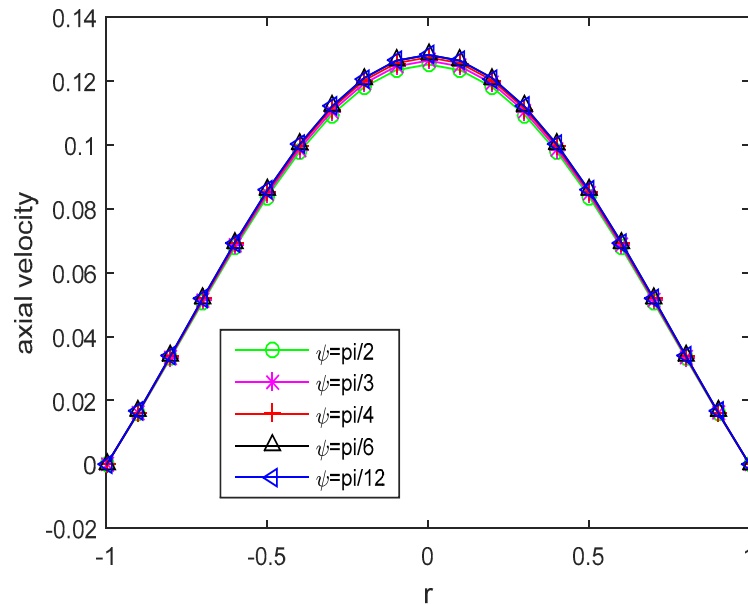


Fig.4. Graph of axial velocity versus  $r$  for various values of the inclination angle  $\psi$  and  $p_0 = 2, p_1 = 4, G_0 = 2, h_1 = 0.4, M = 1.5, t = 1, b = 2, a = 2, \psi = \pi / 3, \phi = 0.25$ .

Figure 5 shows a plot of axial velocity profile versus  $r$  for various values of the slip parameters  $h_1$ . The velocity profile enhances as the values of the slip parameter enhances which is in agreement with the results published in [11, 28]. The effect of body acceleration magnitude  $G_0$  and permeability parameter  $M$  on the axial velocity versus  $r$  in the stenosed portion is shown in Figs 6 and 7. It can be concluded from Fig.6 that when  $G_0$  enhances, the axial velocity profile increases. It can be concluded from Fig.7 that when  $M$  diminishes, i.e.  $k$  increases, the axial velocity increases. Further, it is also observed that parameters  $G_0$  and

$M$  have a great impact on the blood flow in the stenosed region and blood circulation can be increased by increasing and decreasing the parameter  $G_0$  and permeability parameter  $M$ , respectively. Figure 8 shows the trend of velocity profile in three dimensions.

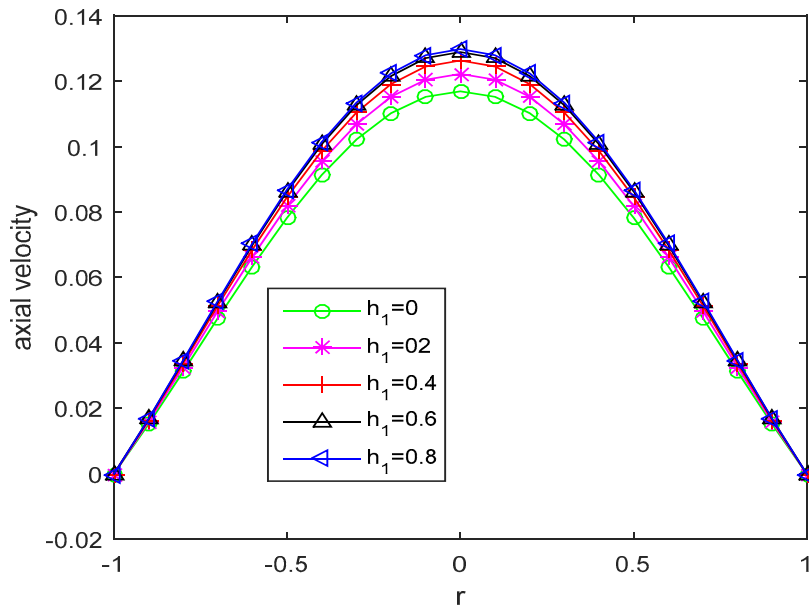


Fig.5. Graph of axial velocity versus  $r$  for various values of the slip parameter  $h_1$  and  $p_0 = 2, p_1 = 4, G_0 = 3, H = 2, M = 1.5, t = 1, b = 2, a = 2, \alpha = 2, \psi = \pi / 3, \phi = 0.25$ .

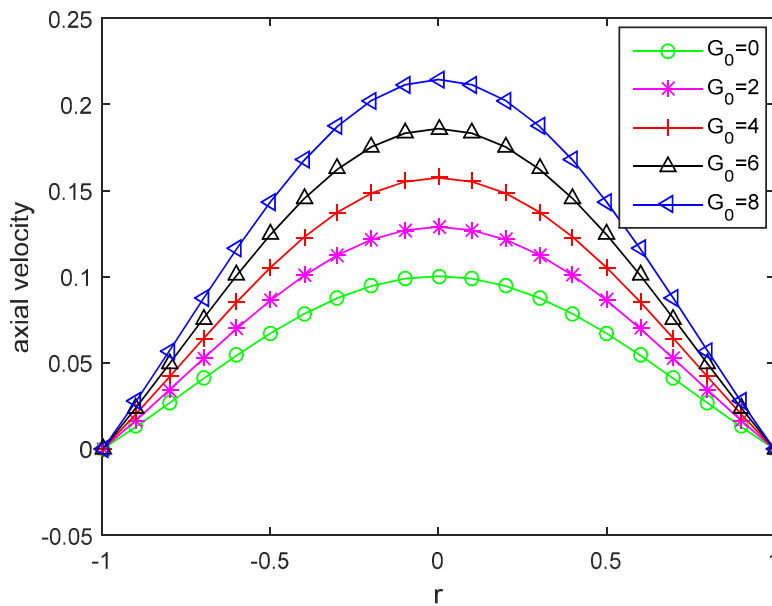


Fig.6. Graph of axial velocity versus  $r$  for various amplitudes of body acceleration  $G_0$  and  $p_0 = 2, p_1 = 4, H = 2, M = 1.5, t = 1, b = 2, a = 2, \alpha = 2, \psi = \pi / 3, h_1 = 0.2, \phi = 0.25$ .

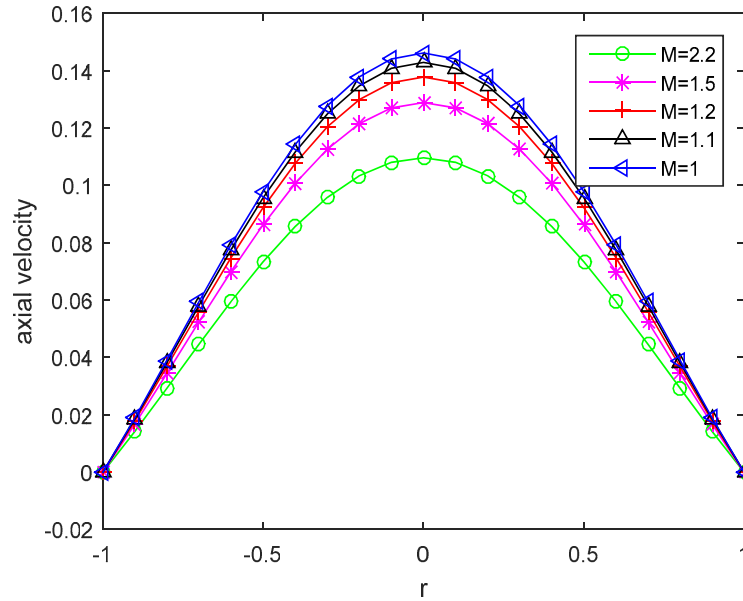


Fig.7. Graph of axial velocity versus  $r$  for various values of the permeability parameter  $M$  and  $G_0 = 2$ ,  $p_0 = 2$ ,  $p_1 = 4$ ,  $H = 2$ ,  $t = 1$ ,  $b = 2$ ,  $a = 2$ ,  $\alpha = 2$ ,  $h_1 = 0.2$ ,  $\psi = \pi / 3$ ,  $\phi = 0.25$ .

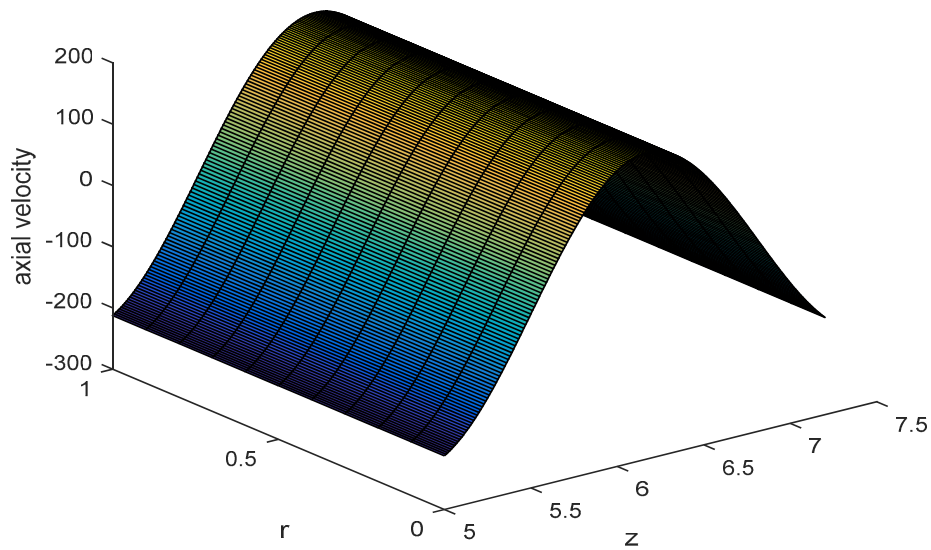


Fig.8. Graph of axial velocity  $u(r,t)$  in three dimensions for  $G_0 = 2$ ,  $p_0 = 2$ ,  $p_1 = 4$ ,  $H = 2$ ,  $M = 1.5$ ,  $t = 1$ ,  $b = 2$ ,  $a = 2$ ,  $\alpha = 2$ ,  $h_1 = 0.2$ ,  $\psi = \pi / 3$ ,  $\phi = 0.25$ .

The variations in blood acceleration  $F(r,t)$  versus time-dependent variant  $t$  of various values of the Hartmann number  $H$  and frequency of body acceleration  $b$  have been displayed in Figs 9 and 10. The figures show that blood acceleration is decreasing with the enhancement of the Hartmann number  $H$  and  $b$  up to  $t = 0.6$ , then it is increasing up to  $t = 1$ . It is also observed that blood acceleration shows a reverse behaviour for  $b = 1$ .

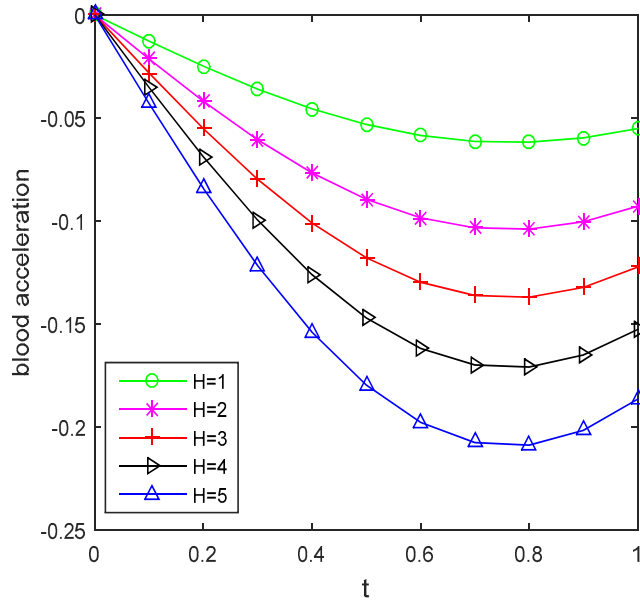


Fig.9. Graph of blood acceleration versus  $t$  for various values of the Hartmann number  $H$  and  $G_0 = 2, p_0 = 2, p_1 = 4, R_0 = 0.4, M = 1.5, b = 2, a = 2, \alpha = 2, h_1 = 0.2, \psi = \pi / 3, \phi = 0.25$ .

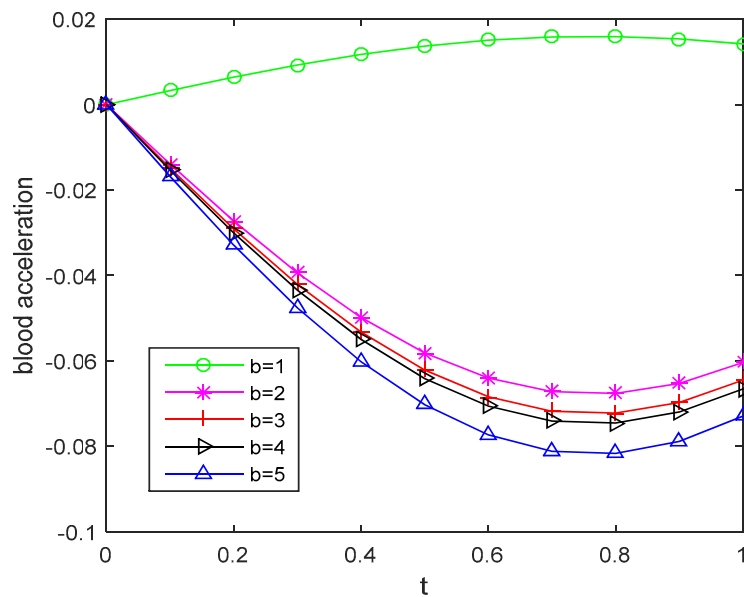


Fig.10. Graph of blood acceleration versus  $t$  for various values of frequency of body acceleration  $b$  and  $p_1 = 4, R_0 = 0.4, G_0 = 2, p_0 = 2, M = 1.5, a = 2, h_1 = 0.2, \alpha = 2, \psi = \pi / 3, \phi = 0.25$ .

Figures 11 and 12 show the profile of blood acceleration for various values of the permeability parameter  $M$ , and Womersley number  $\alpha$ . It is noticed that blood acceleration increases as the amplitude of  $M$  decreases or  $k$  increase and the Womersley number  $\alpha$  increases. Moreover, blood acceleration decreases along  $t$  up to  $t=0.6$ , and then it starts increasing up to  $t = 1$ . The outcomes are similar to the results published in [11, 16].

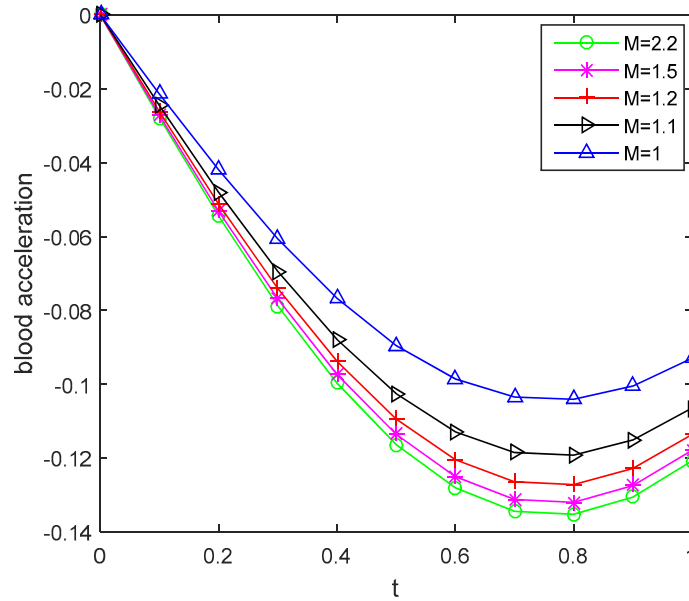


Fig.11. Graph of blood acceleration versus  $t$  for different values of the permeability parameter  $M$  and  $G_0 = 2$ ,  $p_0 = 2$ ,  $p_1 = 4$ ,  $R_0 = 0.4$ ,  $b = 2$ ,  $a = 2$ ,  $h_1 = 0.2$ ,  $\alpha = 2$ ,  $\psi = \pi / 3$ ,  $\phi = 0.25$ .

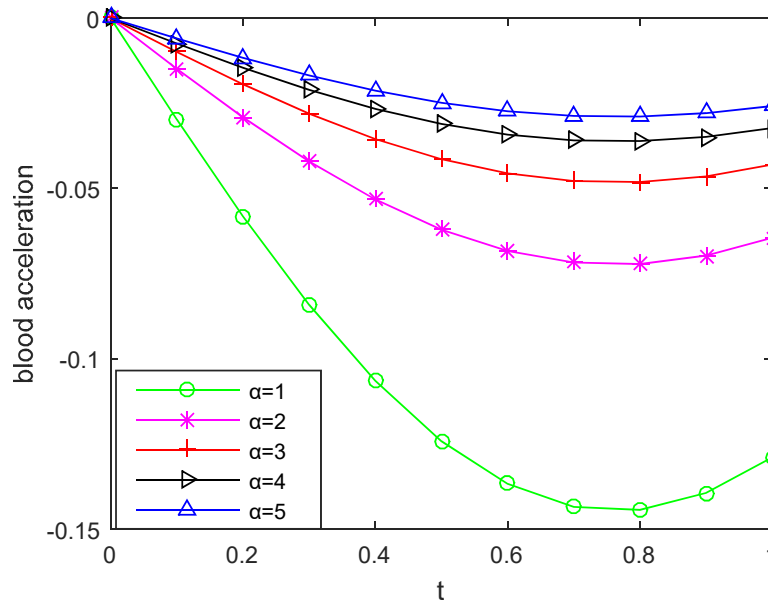


Fig.12. Graph of blood acceleration versus  $t$  for different values of the Womersley parameter  $\alpha$  and  $G_0 = 2$ ,  $p_0 = 2$ ,  $p_1 = 4$ ,  $R_0 = 0.4$ ,  $b = 2$ ,  $a = 2$ ,  $h_1 = 0.2$ ,  $\alpha = 2$ ,  $\psi = \pi / 3$ ,  $\phi = 0.25$ .

Figures 13, 14, and 15 show the variation in  $\tau(r,t)$  versus  $r$  due to the Hartmann number  $H$ , inclination angle  $\psi$ , and visco-elasticity parameter  $\beta$  in the stenosed region of the artery. It is discovered that the shear stress increases with an enhancement of the Hartmann number  $H$ , inclination angle  $\psi$ , and visco-elasticity parameter  $\beta$ . Shear stress has two regions of circulation for  $H < 3$  and  $\beta < 0.6$ . After that, it becomes flattened for  $H = 3$ ,  $H = 4$ , and  $\beta = 0.8, \beta = 1$ . This implies that the intensity of the magnetic field and visco-

elasticity parameter  $\beta$  affect the circulation region. For a large value of the Hartmann number and visco-elasticity parameter  $\beta$ , circulation is observed at the endpoints of the stenosed artery and for small values, circulation happens at the neck of the stenosed artery.

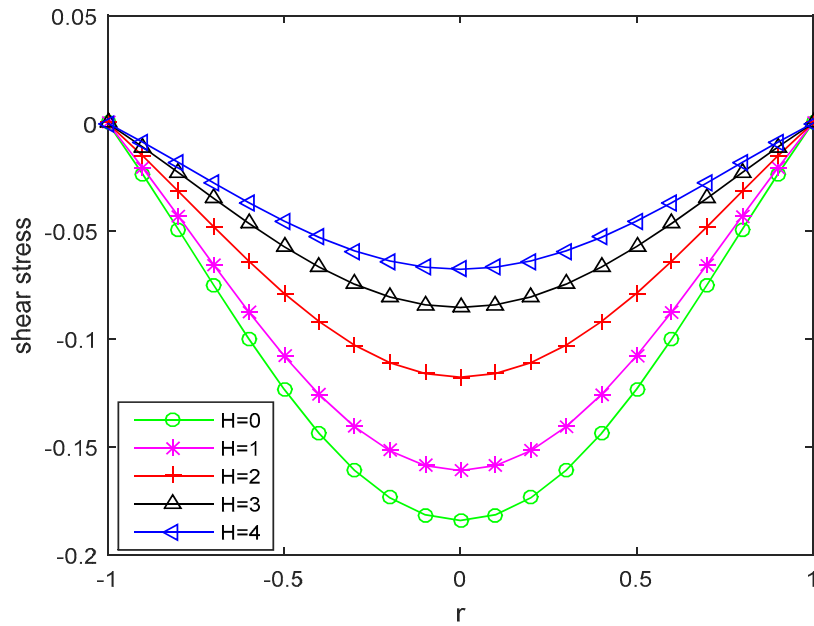


Fig.13. Graph of shear stress  $\tau(r,t)$  versus  $r$  for various values of the Hartmann number  $H$  and  $p_0 = 2$ ,  $p_1 = 4$ ,  $G_0 = 2$ ,  $h_1 = 0.4$ ,  $M = 1.5$ ,  $t = 1$ ,  $b = 2$ ,  $\alpha = 2$ ,  $a = 2$ ,  $\psi = \pi / 3$ ,  $\phi = 0.25$ .

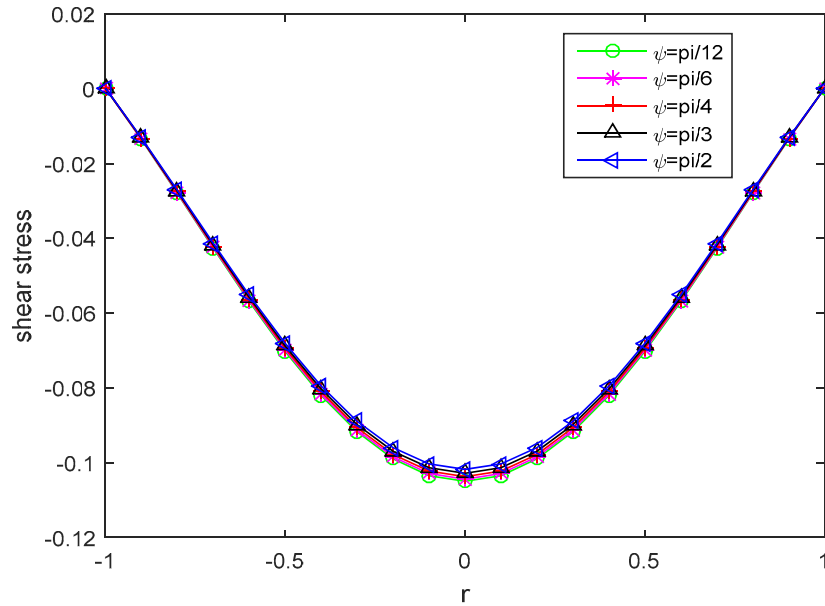


Fig.14. Graph of shear stress  $\tau(r,t)$  versus  $r$  for different values of the inclination angle  $\psi$  and  $p_0 = 2$ ,  $p_1 = 4$ ,  $G_0 = 2$ ,  $h_1 = 0.4$ ,  $M = 1.5$ ,  $t = 1$ ,  $b = 2$ ,  $a = 2$ ,  $\alpha = 2$ ,  $\phi = 0.25$ ,  $H = 2$ .

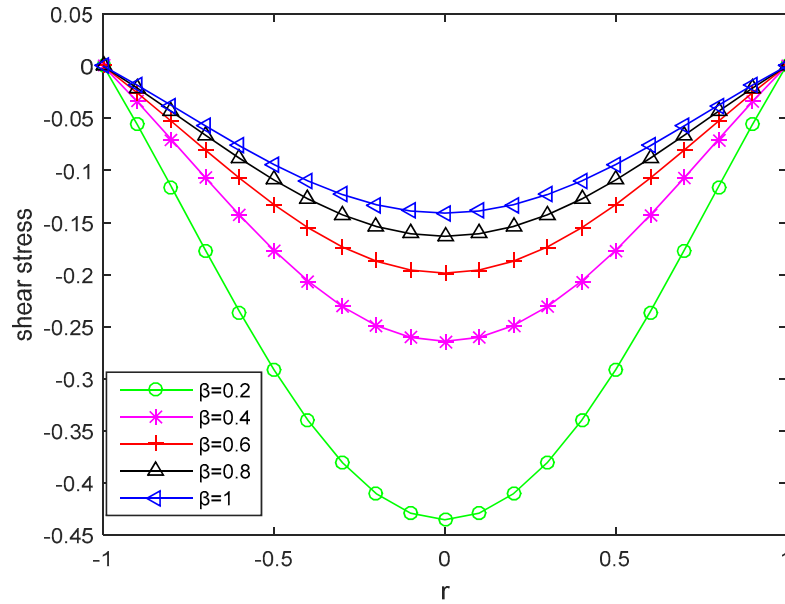


Fig.15. Graph of shear stress  $\tau(r,t)$  versus  $r$  for different values of the visco-elasticity parameter  $\beta$  and  $p_0 = 2, p_1 = 4, G_0 = 2, h_1 = 0.4, M = 1.5, t = 1, b = 2, a = 2, \alpha = 2, \phi = 0.25, H = 2$ .

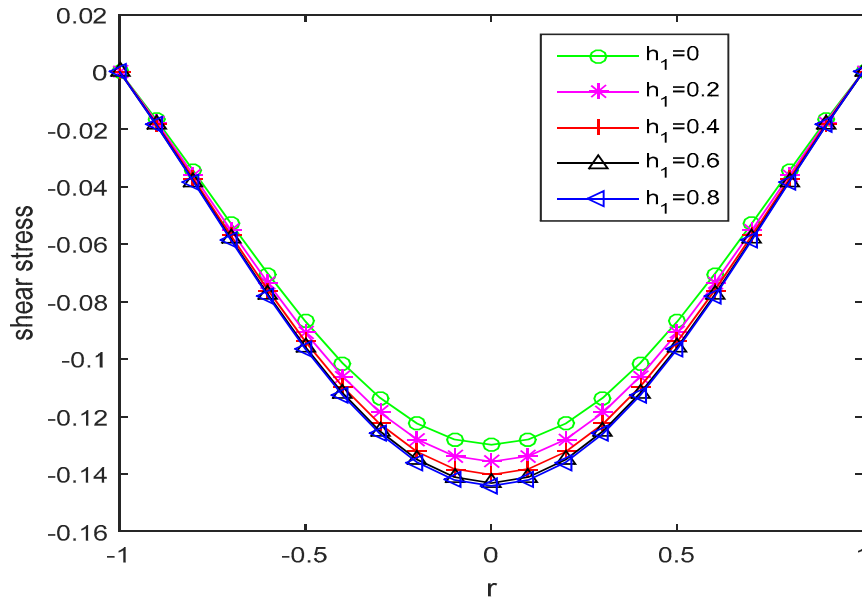


Fig.16. Graph of shear stress  $\tau(r,t)$  versus  $r$  for  $h_1$  and  $p_0 = 2, p_1 = 4, G_0 = 3, H = 2, k = 0.4, t = 1, b = 2, a = 2, \alpha = 2, \psi = \pi / 3, \phi = 0.25$ .

Shear stress for different values of the of body acceleration  $G_0$  and slip parameter  $h_1$  in the stenosed region is displayed in Figs 16 and 17, respectively. As when we enhance the value of  $h_1$  and  $G_0$ , the shear stress profile decreases. Shear stress becomes flattened at  $G_0 = 0$ . The effect of the values of the permeability factor  $M$  on shear stress versus  $r$  in the stenosed region is depicted in Fig.18. It is ascertained from Fig.18 that as the amplitude of  $M$  reduces, i.e.  $k$  increases, the shear stress profile decreases and it becomes flattened

at  $M = 2.2$ . For small values of body acceleration  $G_0$ , slip parameter  $h_1$ , circulation is observed at the endpoints of the stenosed artery and for large values, circulation is observed at the neck of the stenosed artery. The outcomes are similar to the results [16, 21, 25, 11, 28]. The effect of various values of the shear stress in three-dimensions is shown in Fig.19.

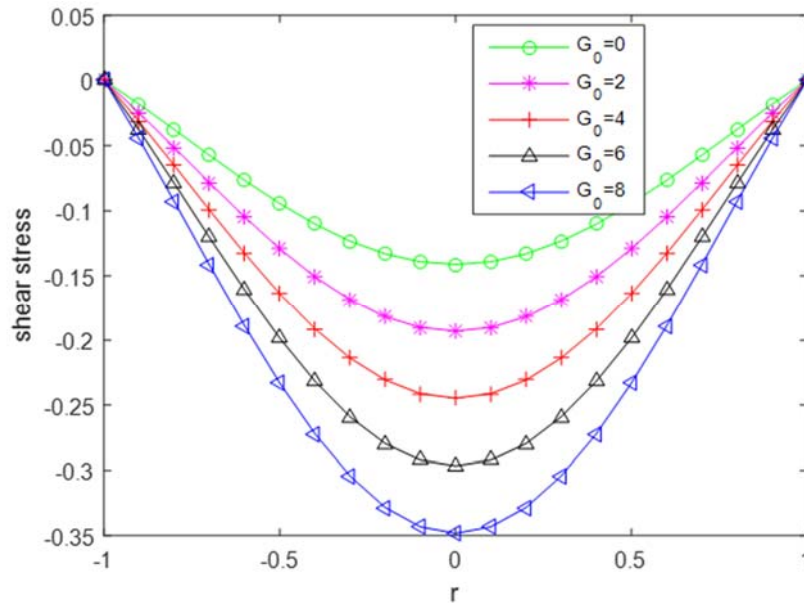


Fig.17. Graph of shear stress  $\tau(r,t)$  versus  $r$  for amplitude of body acceleration  $G_0$  and  $p_0 = 2, p_1 = 4, H = 2, M = 1.5, t = 1, b = 2, a = 2, \alpha = 2, \psi = \frac{\pi i}{3}, h_1 = 0.2, \phi = 0.25$ .

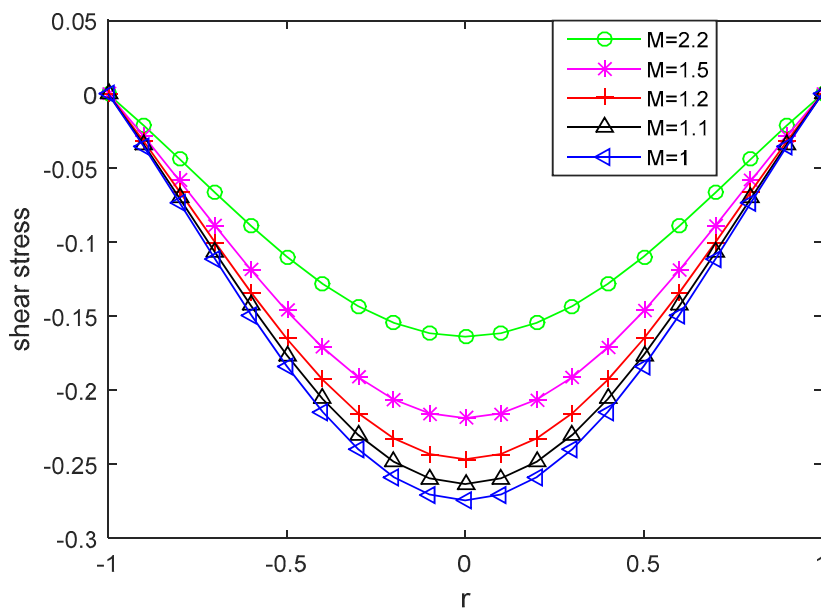


Fig.18. Graph of shear stress  $\tau(r,t)$  versus  $r$  for various values of  $M$  and  $G_0 = 2, p_0 = 2, p_1 = 4, H = 2, t = 1, b = 2, a = 2, \alpha = 2, h_1 = 0.2, \psi = \pi / 3, \phi = 0.25$ .

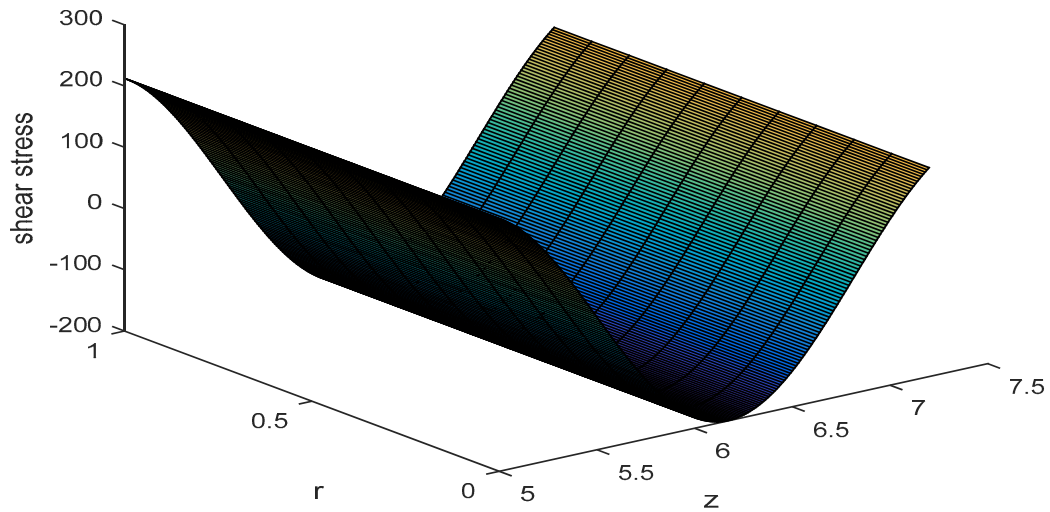


Fig.19. Graph of shear stress  $\tau(r,t)$  in three dimensions for  $G_0 = 2, p_0 = 2, p_1 = 4, H = 2, t = 1, b = 2, a = 2, \alpha = 2, h_1 = 0.2, \psi = \pi / 3, \phi = 0.25$ .

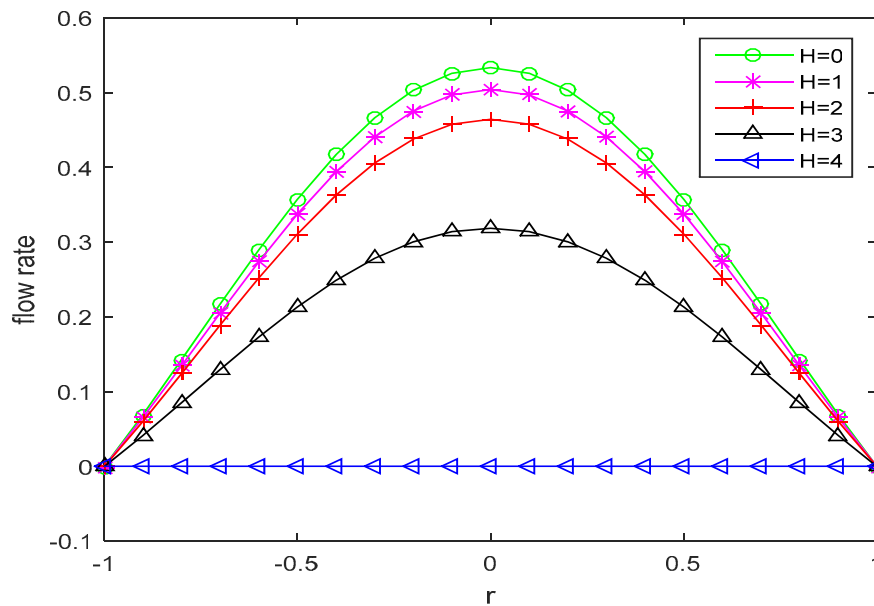


Fig.20. Graph of  $Q$  versus  $r$  for the different values of the Hartmann number  $H$  and  $p_0 = 2, p_1 = 4, G_0 = 2, h_1 = 0.4, M = 1.5, t = 1, b = 2, a = 2, \alpha = 2, \psi = \pi / 3, \phi = 0.25$ .

The trends of flow rate  $Q$  versus  $r$  for different values of the Hartmann number  $H$ , visco-elasticity parameter  $\beta$ , inclination angle  $\psi$ , slip parameter  $h_1$ , the magnitude of body acceleration  $G_0$  are displayed in Figs 20-24. The flow rate reduces as the values of the Hartmann number, inclination angle  $\psi$ , and visco-elasticity parameter  $\beta$  increase and it amplifies with the enhancement of  $h_1$ , and  $G_0$ . The trend of flow rate  $Q$  versus  $r$  for the permeability parameter  $M$  is displayed in Fig.25. The flow rate amplifies as the value of

the permeability parameter  $M$  decreases, i.e.  $k$  increases. The trend of flow rate  $Q$  in three dimensions is illustrated in Fig.26.

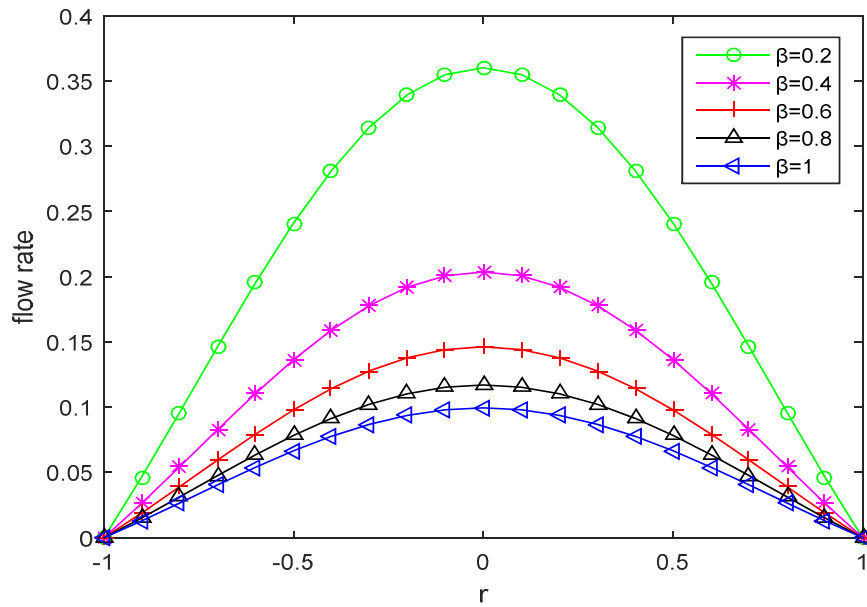


Fig.21. Graph of  $Q$  versus  $r$  for different values of the visco-elasticity parameter  $\beta$  and  $p_0 = 2, p_1 = 4, G_0 = 2, h_1 = 0.4, M = 1.5, t = 1, b = 2, a = 2, \alpha = 2, \psi = \pi / 3, \phi = 0.25$ .

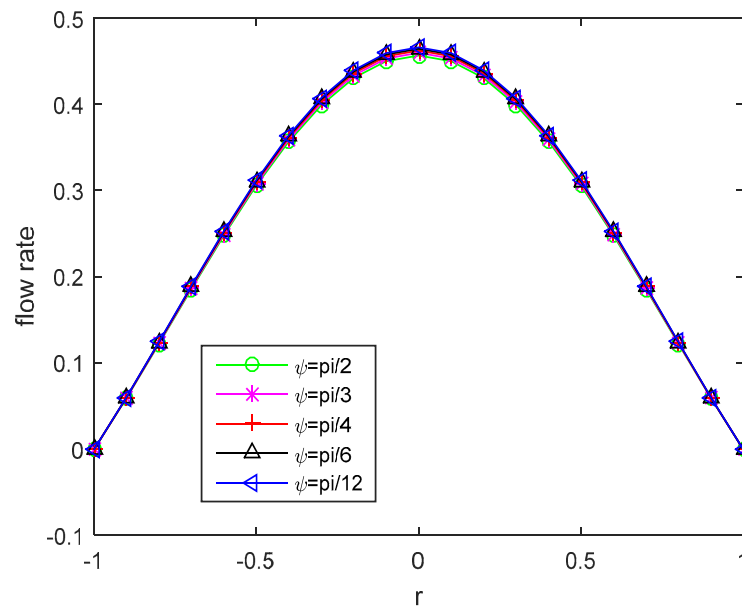


Fig.22. Graph of  $Q$  versus  $r$  for different values of the inclination angle  $\psi$  and  $p_0 = 2, p_1 = 4, G_0 = 2, h_1 = 0.4, M = 1.5, t = 1, b = 2, a = 2, \alpha = 2, \phi = 0.25, H = 2$ .

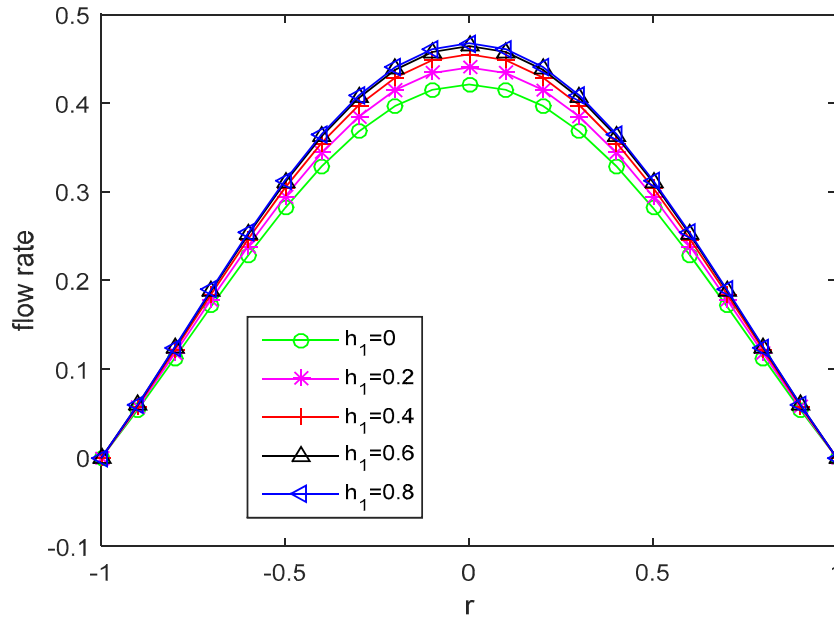


Fig.23. Graph of  $Q$  versus  $r$  for the different values of  $h_1$  and  $p_0 = 2, p_1 = 4, G_0 = 3, H = 2, M = 1.5, t = 1, b = 2, a = 2, \alpha = 2, \psi = \pi / 3, \phi = 0.25$ .

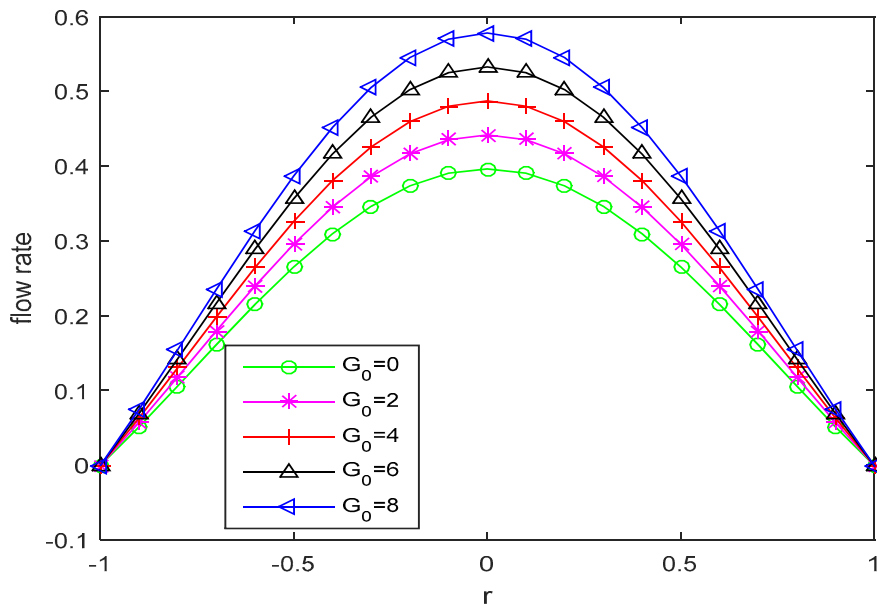


Fig.24. Graph of  $Q$  versus  $r$  for different values of body acceleration  $G_0$  and  $p_0 = 2, p_1 = 4, H = 2, M = 1.5, t = 1, b = 2, a = 2, \alpha = 2, \psi = \pi / 3, h_1 = 0.2, \phi = 0.25$ .

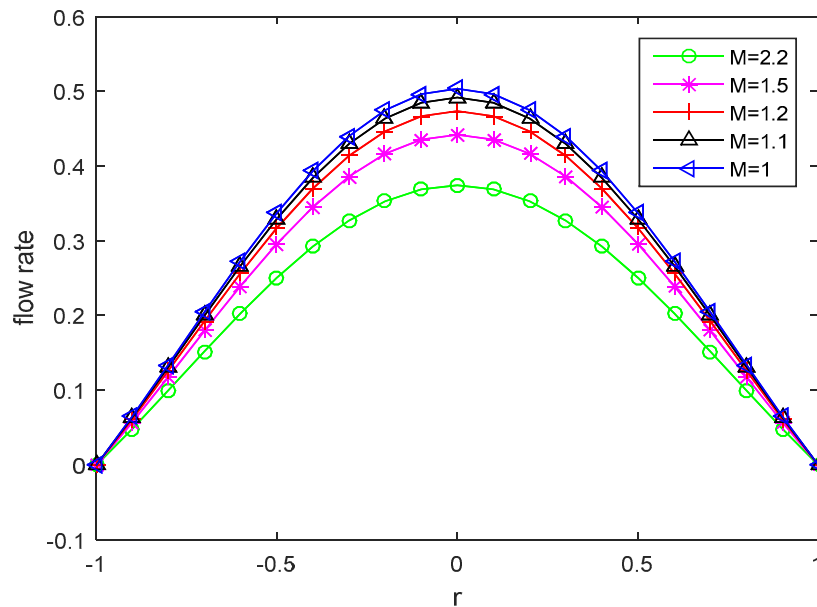


Fig.25. Graph of  $Q$  versus  $r$  for different values of  $M$  and  $G_0 = 2, p_0 = 2, p_1 = 4, H = 2, t = 1, b = 2, a = 2, \alpha = 2, h_1 = 0.2, \psi = \pi / 3, \phi = 0.25$ .

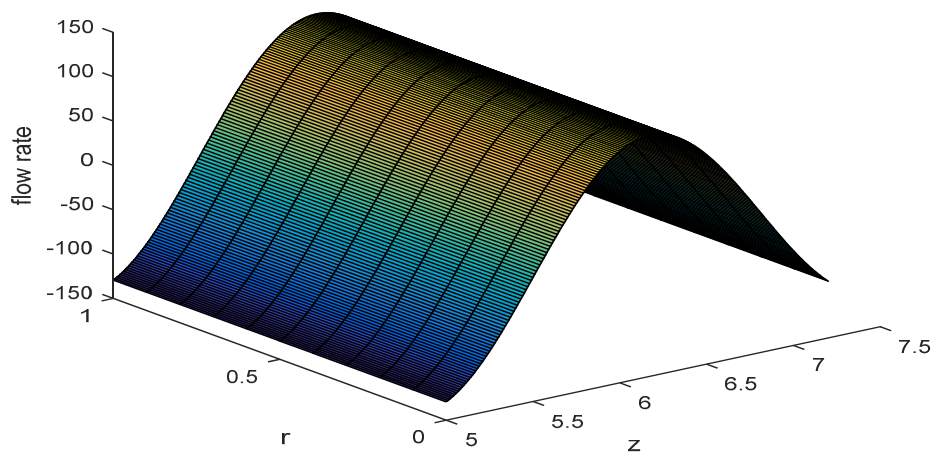


Fig.26. Graph of flow rate  $Q$  in three dimensions  $G_0 = 2, p_0 = 2, p_1 = 4, H = 2, M = 1.5, t = 1, b = 2, a = 2, h_1 = 0.2, \alpha = 2, \psi = \pi / 3$  and  $\phi = 0.25$ .

### 7. Conclusion

In the present work, an MHD unsteady blood flow in an inclined porous stenosed artery is examined. This work is also useful for assessing the role of porosity. The study has been performed by using a suitable analytical method and some appropriate assumptions were made. Some important observations of the present work have been given below as:

1. Axial velocity reduces as the value of the Hartmann number, inclination angle and visco-elasticity parameter are increasing but it enhances as the slip parameter and magnitude of body acceleration are

- enhancing. Thus, blood velocity could be managed by using a relevant magnetic field. It can be enhanced by the permeability parameter.
2. Blood acceleration reduces as the value of the Hartmann number, and body acceleration frequency are increasing and it enhances as the value of the Womersley number is increasing. Blood acceleration is also increasing with the permeability parameter.
  3. Shear stress enhances while the values of the Hartmann number, visco-elasticity parameter and inclination angle are growing and it decreases as the value of the slip parameter and the magnitude of body acceleration are enhancing. Shear stress also decreases with the permeability parameter.
  4. Flow rate reduces as the values of the Hartmann number, inclination angle and visco-elasticity parameter are increasing but it enhances as slip parameter, and magnitude of body acceleration are enhancing. Thus, flow rate could be managed by using a relevant magnetic field. Flow rate enhances with the permeability parameter.

The present study will be useful in medical research for the analysis of cardiovascular diseases through magnetic therapy. Understanding of blood acceleration could be helpful in the remedial analysis of some health complications like inflammation of the joint, vascular disorder, and blurred vision.

### Acknowledgment

This work is affiliated with the Department of Applied Sciences, University Institute of Engineering and Technology, Maharshi Dayanand University, Rohtak, Haryana, INDIA, and is supported by Maharshi Dayanand University, Rohtak, Haryana, INDIA.

### Nomenclature

$f_p$	– oscillations of a heart pulse
$f_b$	– frequency of body acceleration
$G_0$	– magnitude of body acceleration
$H$	– Hartmann number
$Hm$	– greatest concentration of hematocrit
$h(r)$	– concentration of hematocrit
$L$	– half artery length
$L_0$	– half stenosis length
$M$	– permeability parameter
$p_0$	– pressure gradient of steady portion
$p_1$	– oscillatory pressure gradient
$R_0$	– normal artery radius
$R(z)$	– stenosed artery radius
$\alpha$	– Womersley parameter
$\mu_0$	– viscosity coefficient
$\beta$	– constant
$\delta$	– extreme stenosis depth
$\mu_1$	– coefficient of visco-elastic fluid
$\phi$	– phase difference
$\psi$	– inclination angle of the arterial segment

### References

- [1] Cowling T.G. (1957): *Magnetohydrodynamics*.– Interscience Publishers, New York.

- [2] Beaver G.S. and Joseph D.D. (1967): *Boundary conditions at a naturally permeable wall.*– Journal of Fluid Mechanics, vol.30, pp.197-207.
- [3] Saffman P. D. (1971): *On the boundary conditions at the surface of porous medium.*– Study of Applied Mathematics, vol.50, pp.93-101.
- [4] Chaturani P. and Biswas D. (1984): *A comparative study of poiseuille flow of a polar fluid under various boundary conditions with applications to blood flow.*– Rheologica Acta, vol.23, No.4, pp.435-445.
- [5] Elshehawey E.F., Elbarbary E.M.E. Afifi N.A.S. and Elshahed M. (1999): *MHD flow of an visco-elastic fluid under periodic body acceleration.*– International. Journal Mathematics & Mathematical Sciences, vol.23, No.11, pp.795-799.
- [6] Tzirtzilakis E.E. (2005): *A mathematical model for blood flow in magnetic field.*– Physics of Fluid, vol.17, No.7, Article ID 077103, pp.1-15.
- [7] El-Shehawey EF., El-Debe N.T. and El-Desoky I.M. (2006): *Slip effects on the peristaltic flow of a non-Newtonian Maxwellian fluid.*– Acta Mechanica, vol.186, pp.141-159.
- [8] Ponalagusamy (2007): *Blood flow through an artery with mild stenosis: A two-layered model, different shape of stenosis and slip velocity at wall.*– Journal of Applied Science, vol.7, pp.1071-1077.
- [9] Nagarani P. and Sarojamma G. (2008): *Effect of body acceleration on pulsatile flow of Casson fluid through a mild stenosed artery.*– Korea-Australia Rheology Journal, vol.20, pp.189-196.
- [10] Hayat T., Hussain Q. and Ali N. (2008): *Influence of partial slip on the peristaltic flow in porous medium.*– Physica A, vol.387, No.14, pp.3399-3409.
- [11] Rathod V.P. and Tanveer S. (2009): *Pulsatile flow of couple stress fluid through porous medium with periodic body acceleration and magnetic field.*– Bulletin of Malaysian Mathematical Society Series, vol.32, pp.245-259.
- [12] Verma N. and Parihar R. S. (2009): *Effects of magneto-hydrodynamic and hematocrit on blood flow in very narrow capillaries.*– International Journal of Applied Mathematics and Computation, vol.1, No.1, pp.30-46.
- [13] Nadeem S. and Akram S. (2010): *Slip effects on the peristaltic flow of a Jeffrey fluid in an asymmetric channel under the effect of an induced magnetic field.*– International Journal for Numerical Methods in Fluids, vol.63, No.3, pp.374-394.
- [14] Sinha A., Misra J.C. and Shit J. C. (2010): *Mathematical modeling of blood flow with variable viscosity through an intended artery due to an LDL effect in the presence of magnetic field.*– International Journal of Physical Sciences, vol.5, No.12, pp.1857-1868.
- [15] Chakraborty U.S., Biswas, D. and Paul M. (2011): *Suspension model blood flow through an inclined tube with an axially non-symmetrical stenosis.*– Korea-Australia Rheology Journal, vol.23, No.1, pp.25-32.
- [16] Eldesoky I.M. (2012): *Slip effects on the unsteady MHD pulsatile blood flow through porous medium in an artery under the effect of body acceleration.*– International Journal of Mathematics and Mathematical Sciences, Article ID 860239, p.26.
- [17] Tripathi (2012): *A mathematical model for blood flow through an inclined artery under the influence of an inclined magnetic field.*– Journal of Mechanics in Medicine and Biology, vol.12, pp.1-18.
- [18] Sharma M.K., Bansal K. and Bansal S. (2012): *Pulsatile unsteady flow of blood through porous medium in a stenotic artery under the influence of transverse magnetic field.*– Korea-Australia Rheology Journal, vol.24, No.3, pp.181-189.
- [19] Sinha A., Shit G.C. and Kundu P.K. (2013): *Slip effect on pulsatile flow of blood through a stenosed arterial segment under periodic body acceleration.*– ISRN Biomedical Engineering, vol.2013, Article ID 925876, p.10.
- [20] Sharma M. Sharma P. and Nasha V. (2013): *Pulsatile MHD arterial blood flow in the presence of double stenoses.*– Journal of Applied Fluid Mechanics, vol.6, No.3, pp.331-338.
- [21] Eldesoky I.M.I. (2014): *Unsteady MHD pulsatile blood flow through porous medium in stenotic channel with slip at permeable walls subjected to time-dependent viscosity (injection/suction).*– Walailak Journal of Science and Technology, vol.11, No.11, pp.901-922.
- [22] Sharma M. Singh K. and Bansal S. (2014): *Pulsatile MHD flow in an inclined catheterized stenosed artery with slip on the wall.*– Journal of Biomedical Science and Engineering, vol.7, pp.194-207.
- [23] Srivastava N. (2014): *Analysis of flow characteristics of the blood flowing through an inclined tapered porous artery with mild stenosis under the influence of an inclined magnetic field.*– Journal of Biophysics, Article ID 797142, p.9.

- [24] Sharma M., Sharma P. and Nasha V. (2015): *Pulsatile blood flow through stenosed artery with axial translation.*– International Journal of Biomathematics, vol.8, No.3, 1550028, p21.
- [25] Kumar A., Chandel R.S., Shrivastava R., Shrivastava K. and Kumar S. (2016): *Mathematical modelling of blood flow in an inclined tapered artery under MHD effect through porous medium.*– International Journal of Pure and Applied Mathematical Sciences, vol.9(1), pp.75-88.
- [26] Sharma M., Nasha V. and Sharma P. (2016): *A study for analyzing the effect of overlapping stenosis and dilatation on non-Newtonian blood flow in an inclined artery.*– Journal of Biomedical Science and Engineering, vol.9, pp.576-596.
- [27] Chitra M. and Karthikeyan D. (2018): *Unsteady MHD oscillatory blood flow in an inclined tapered artery with mild stenosis through porous medium: effects of slip velocity.*– International Journal of Mathematics Trend and Technology (IJMTT)-special issue NCCFQET, pp.44-49.
- [28] Kumari S., Rathee R. and Nandal J. (2019): *Unsteady peristalsis transport of MHD fluid through an inclined stenosed artery with slip effects.*– International Journal of Applied Engineering research, vol.24, No.3, pp.645-659.
- [29] Manisha, Nasha V. and Kumar S. (2021): *MHD Two-layered blood flow under effect of heat and mass transfer in stenosed artery with porous medium.*– International Journal of Advance Research in Engineering and Technology, vol.12, No.6, pp.63-76.
- [30] Jaafar N.A., Zainulabidin S.N.M., Ismail Z. and Mohamad A.Q. (2021): *Mathematical analysis of unsteady solute dispersion with chemical reaction through a stenosed artery.*– Journal of Advanced Research in Fluid Mechanical and Thermal Science, vol.86, No.2, pp.56-73.
- [31] Shah N.A. Zubaidi A.A.I. and Saleem S. (2021): *Study of magneto-hydrodynamic pulsatile blood flow through an inclined porous cylindrical tube with generalized time-nonlocal shear.*– Advance in Mathematical Physics, article Id 5546701, p.11.
- [32] Manisha Nasha V. and Kumar S. (2022): *Non-newtonian blood flow model with the effect of different geometry of stenosis.*– Journal of Mathematical and Computational Sciences, vol.12, pp.1-21.
- [33] Manisha and Kumar S. (2022): *Effect of cosine shape stenosis on non-newtonian blood flow with Casson model in stenosed artery.*– International Journal of Engineering Trends and Technology, vol.70, No.8, pp.336-346.

Received: July 26, 2022

Revised: October 21, 2022